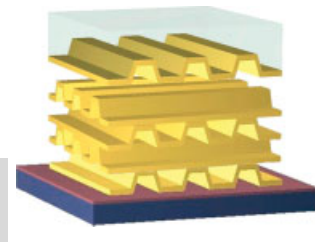


# Three-Dimensional Nanofabrication with Rubber Stamps and Conformable Photomasks\*\*

By *Seokwoo Jeon, Etienne Menard, Jang-Ung Park, Joana Maria, Matthew Meitl, Jana Zaumseil, and John A. Rogers\**



*This article briefly describes two recently developed soft-lithographic techniques that can be used to fabricate complex, well-defined three-dimensional (3D) nanostructures. The first relies on the single or multilayer transfer of thin solid 'ink' coatings from high-resolution rubber stamps. The second uses these stamps as conformable phase masks for proximity field nanopatterning of thin layers of transparent photopolymers. Although both techniques use the same pattern-transfer elements, they rely on completely different physical principles and they provide complementary patterning capabilities. The operational simplicity of the techniques, their ability to pattern large areas quickly, and the flexibility in the geometry of structures that can be formed with them suggest general utility for 3D nanomanufacturing.*

## 1. Introduction

Advances in nanoscience and technology rely strongly on techniques for fabricating structures with nanometer dimensions. Methods developed in the microelectronics industry—photolithography, electron-beam lithography, and others—are well suited for patterning two-dimensional (2D) structures on ultraflat glass or semiconductor surfaces. It is challenging, however, to fabricate with them the types of three-dimen-

sional (3D) nanostructures that are important for many areas of nanotechnology. The repetitive patterning of 2D structures on a single substrate provides an indirect route to 3D structures. This strategy, however, requires sophisticated facilities and is difficult to implement for structures that demand more than a few layers. We<sup>[1–5]</sup> and others are interested in alternative methods. Techniques based on colloidal sedimentation,<sup>[6–8]</sup> polymer phase separation,<sup>[9–13]</sup> templated growth,<sup>[14–17]</sup> fluidic assembly,<sup>[17–19]</sup> interference lithography,<sup>[20,21]</sup> writing, embossing, etc.<sup>[22–24]</sup> all provide alternative approaches to certain types of 3D nanostructures. We recently developed two soft-lithographic techniques for 3D patterning. The first, which we refer to as nanotransfer printing (nTP), uses surface chemistries as interfacial “glues” and “release” layers to control the transfer of solid material coatings from relief features on a stamp to a substrate.<sup>[1–4]</sup> The second, which we refer to as proximity field nanopatterning (PnP), uses these stamps as conformable phase masks for directly defining 3D structures in thick, transparent layers of photopolymers.<sup>[5]</sup>

## 2. Nanotransfer Printing

Nanotransfer printing is conceptually similar to microcontact printing ( $\mu$ CP)<sup>[25]</sup>—the first soft-lithographic technique

[\*] Prof. J. A. Rogers, S. Jeon, E. Menard, J.-U. Park, J. Maria, M. Meitl  
Department of Materials Science and Engineering  
and Department of Chemistry  
Seitz Materials Research Laboratory and Beckman Institute  
University of Illinois at Urbana-Champaign  
Urbana, IL 61801 (USA)  
E-mail: jrogers@uiuc.edu  
Dr. J. Zaumseil  
Bell Laboratories, Lucent Technologies  
Murray Hill, NJ 07974 (USA)

[\*\*] We wish to thank our past and current collaborators at Harvard University and Bell Laboratories for the joint efforts described here. This material is based upon work partially supported by the U.S. Department of Energy, Division of Materials Sciences under Award No. DEFG02-91ER45439, through the Frederick Seitz Materials Research Laboratory and the Center for Microanalysis of Materials at the University of Illinois at Urbana-Champaign.

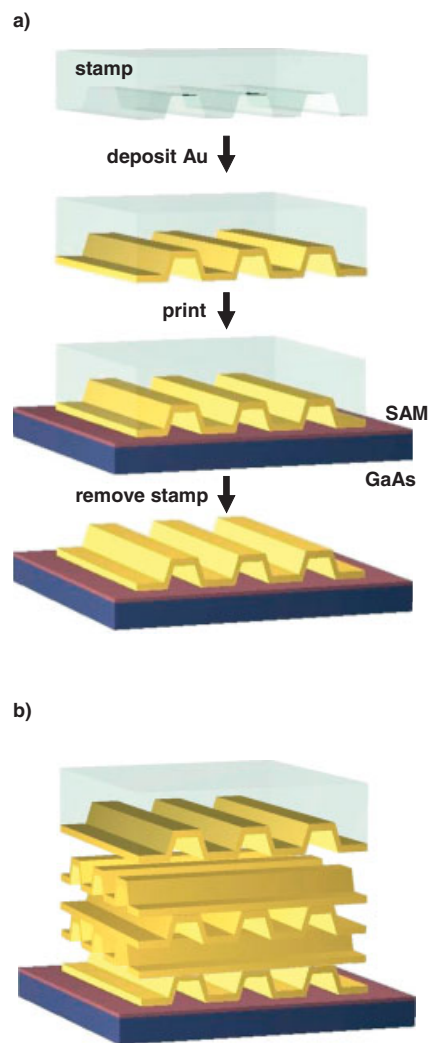
developed by Whitesides and co-workers—in the sense that high-resolution stamps are used to generate patterns in the geometry of their relief structure. However, instead of printing thiol “inks” onto Au films, as in the most common form of  $\mu$ CP, nTP (in one example) prints Au films onto thiol-terminated monolayers. This approach is purely additive (i.e., material is only deposited in locations where it is needed) and it can generate complex two- or three-dimensional structures in single or multiple layers with nanometer resolution. Elastomeric stamps similar those of  $\mu$ CP as well as stamps of hard, inorganic materials can be used. This method has been explored by our group, and, in independent efforts on related techniques, by several other groups.<sup>[26–29]</sup>

Figure 1 illustrates the procedures for printing single and multilayer 3D nanostructures with nTP.<sup>[3,4]</sup> In the first step, a conformal layer of Au is deposited by physical vapor deposition onto the surface of the stamp. Contacting this stamp with a substrate that supports a suitable surface chemistry results in covalent bonding between the Au coating and the substrate. In the example of Figure 1a, a monolayer of octanedithiol on a GaAs substrate provides exposed thiol groups that can bond to the Au coating when the stamp contacts the substrate.<sup>[30]</sup> If the surface of the stamp is treated such that the coating does not adhere well to it, then removing the stamp leaves a pattern with the geometry of the relief features. An array of sealed nanochannels results from the printing in the example of Figure 1a. Printing multiple times with a similar stamp yields stacks of such nanochannels, as illustrated in Figure 1b.<sup>[3]</sup> In this case, Au–Au cold welding<sup>[31]</sup> bonds one channel array to another. Figure 2 presents scanning electron microscope (SEM) images of a variety of 3D nanostructures formed by nTP. Single layers of nanochannels and integrated micro/nanochannel systems (Fig. 2a), as well as large stacks of nanochannels (Fig. 2b), are possible.<sup>[3,4]</sup> Other structures that would be difficult to fabricate in conventional ways can also be built: arrays of sealed nanocapsules (Figs. 2c,d) and free-standing “L”-shaped features (Figs. 2e,f). The latter structures were fabricated with a stamp coated with Au using a flux oriented at a steep angle to the surface of the stamp.<sup>[4]</sup> All of these examples shown in Figure 2 are made of thin (20 nm) Au.

nTP offers much higher resolution than  $\mu$ CP, and it also provides some unique 3D patterning capabilities. Its processing windows, however, are narrower than those of  $\mu$ CP. There are at least three aspects that are important to achieving high fidelity with nTP.<sup>[4]</sup>

- the deposition procedures must be carefully controlled to avoid cracking or buckling of the metal films when poly(dimethylsiloxane) (PDMS) stamps are used,
- PDMS stamps must be handled carefully before and during the printing to avoid surface strains that can damage the metal coatings, and
- the surface chemistry must provide a high density of bonding sites, and the stamps and substrates must come into uniform, intimate contact to allow efficient transfer.

For the first issue, high deposition rates and surface treatments that facilitate wetting of the metals on the surfaces of



**Figure 1.** a) A schematic illustration of procedures for using nanotransfer printing to fabricate 3D nanostructures. Coating a high-resolution stamp with a thin layer of Au prepares the stamp for printing. Contact with a substrate that presents a surface chemistry that bonds to the Au, followed by removal of the stamp (to which the Au does not adhere well) transfers the Au from the stamp to the substrate. The example illustrated here produces arrays of sealed nanochannels bonded to a GaAs wafer with an octanedithiol self-assembled monolayer (SAM). Additional printing steps generate stacks of such nanochannels, as shown in part (b). Au–Au cold welding bonds these layers.

the stamps are important. For the second, composite stamp designs that use rigid backings and relatively thin PDMS layers are helpful. These same stamps also prevent in-plane distortions that can frustrate multilevel registration. In the case of the third issue, suitable chemistries must be employed with substrates that present a low degree of roughness. We have demonstrated gold–gold cold welding, surface hydroxyl chemistries, and thiol-based self-assembled monolayers (SAMs) for inducing the transfer.<sup>[1–4,30]</sup> With well-controlled procedures, patterns over large areas (several square centimeters) that are free of defects or cracks (as observed by high-resolution scanning electron and atomic force microsc-

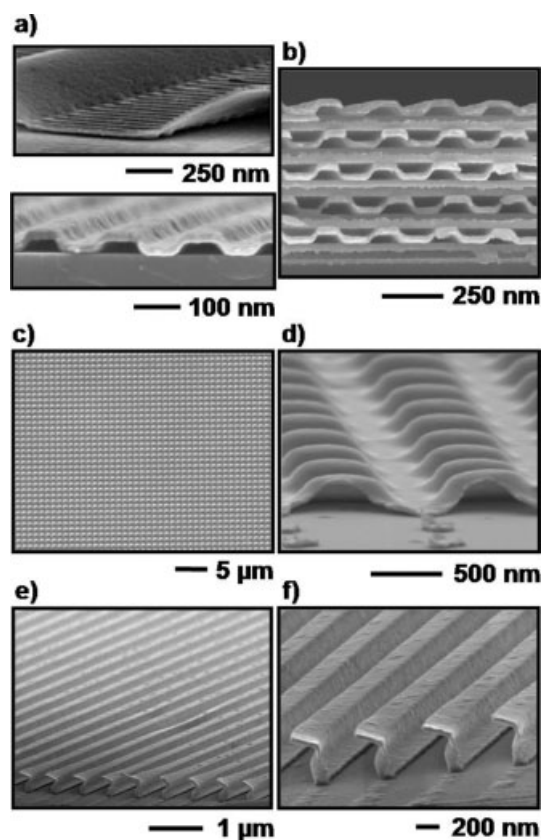


**Figure 2.** Scanning electron micrographs of 3D nanostructures formed by nanotransfer printing. a) Arrays of nanochannels and integrated micro/nanochannel systems. b) A ten layer stack of crossed nanochannels. c,d) Low- and high-resolution images of a square array of sealed nanocapsules. e,f) Low- and high-resolution images of an array of free standing "L"-shaped structures formed by printing with a stamp that is coated with Au at a steep angle. All of these structures are made of thin (20 nm) layers of Au.

py) can be produced.<sup>[4]</sup> In many cases, a residual, ultrathin layer of organic material transfers with the metal film when PDMS stamps are used. This layer is on the order of 1–4 nm thick, depending on the processing conditions. It can be removed using dry or wet etching.<sup>[4]</sup>

### 3. Proximity Field Nanopatterning

A second soft-lithographic approach to 3D nanofabrication uses PDMS stamps as conformable phase masks.<sup>[5]</sup> Here, the same van der Waals' wetting interactions that bring a stamp into contact with a flat surface are used to establish atomic-scale contact between a mask with a layer of photosensitive material. Passing light through the mask exposes the layer to the distribution of intensity that develops near the surface of the mask.<sup>[32–36]</sup> Figure 3a provides a schematic illustration of a PDMS mask that has a single step edge of relief with a depth that modulates the phase of the transmitted exposure light by  $\pi$ . A sharp shadow (i.e., null in the intensity) develops at the

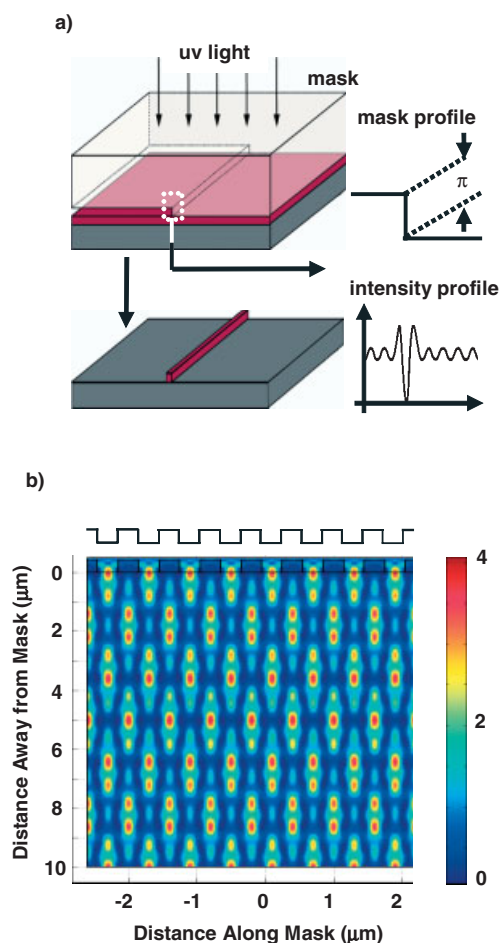


**Figure 3.** a) A schematic illustration of near-field exposure of a thin layer of positive resist with a conformable phase mask. A step edge of relief with a depth suitable for modulating the optical phase by  $\pi$  leads to a phase shadow with a characteristic width of  $\sim 100$  nm for 365 nm exposure light. Developing the resist yields a line with a similar width. b) Finite-element modeling of the passage of a plane wave through a mask that presents relief features with widths comparable to the optical wavelength. This distribution of intensity can be used for fabricating 3D nanostructures in thick, transparent layers of photopolymers.

surface of the mask in this case.<sup>[33]</sup> Simple scalar diffraction modeling of this effect appears in Figure 3a. The characteristic width of this shadow is  $\sim 100$  nm when the 365 nm light from a mercury lamp is used. Exposing and fully developing a thin layer of positive photoresist in this manner generates line structures with widths of 50–100 nm. Two consecutive exposures with a rotation of the stamp in between can generate posts. Partial development of the resist can reproduce some of the fine-scale features (i.e., the oscillations) of the intensity distributions (Fig. 3a) in shapes of resist that have some modest 3D structure.

Full vector solutions to Maxwell's equations show that an array of step edges separated by a distance that is comparable to the wavelength of the exposure light creates a periodic distribution of intensity, with peaks in the intensity at the raised regions of the mask.<sup>[5]</sup> An important feature of the optics is

that this distribution of intensity varies in a regular fashion not only along the surface of the mask but also in the direction normal to its surface, provided that the light has sufficient coherence. Figure 3b shows the results of finite element computations when normally incident plane waves with wavelength 365 nm pass through a mask with binary relief features that are 300 nm wide and 420 nm deep. This general optical effect (which is present in various forms with masks that have aperiodic as well as periodic features) can be exploited for 3D nanofabrication by exposing thick layers of transparent photopolymers and then developing them (to remove the unexposed or exposed regions, depending on the photochemistry).

Figure 4 shows some structures formed by these near and proximity field patterning techniques. The small features in Figure 4a (single exposure) and Figure 4b (double exposure) result from near-field exposure and full development. Quasi-3D structures result from partial development, as illustrated in the images and simulations of Figures 4c,d. Full 3D nanostructures of Figure 4e are produced by proximity mode exposure using a subwavelength phase mask and a transparent photopolymer that crosslinks in the exposed regions. The right frame of Figure 4g shows numerical modeling of the intensity distribution; it quantitatively reproduces the key features of the structures. The smallest features in these types of patterns have dimensions of 50–100 nm.

#### 4. Concluding Remarks

In summary, this article summarizes two recent soft-lithographic techniques that combine nanometer resolution with the ability to pattern 3D features. Several examples illustrate some of types of structures that can be constructed. New chemistries and processing techniques will enable direct patterning of other classes of materials. The use of patterned structures as sacrificial templates can generate replicas out of materials that are difficult to pattern directly. Anticipated applications span a wide range of research and development areas in nanotechnology, including photonics (thin holographic correlators, unusual filters, plasmonic devices, etc.), sensors (e.g., high surface area optical systems, surfaces for enhanced Raman scattering, etc.), fluidics (passive mixers, filters, media for chromatographic separations, etc.), and high-density storage systems.

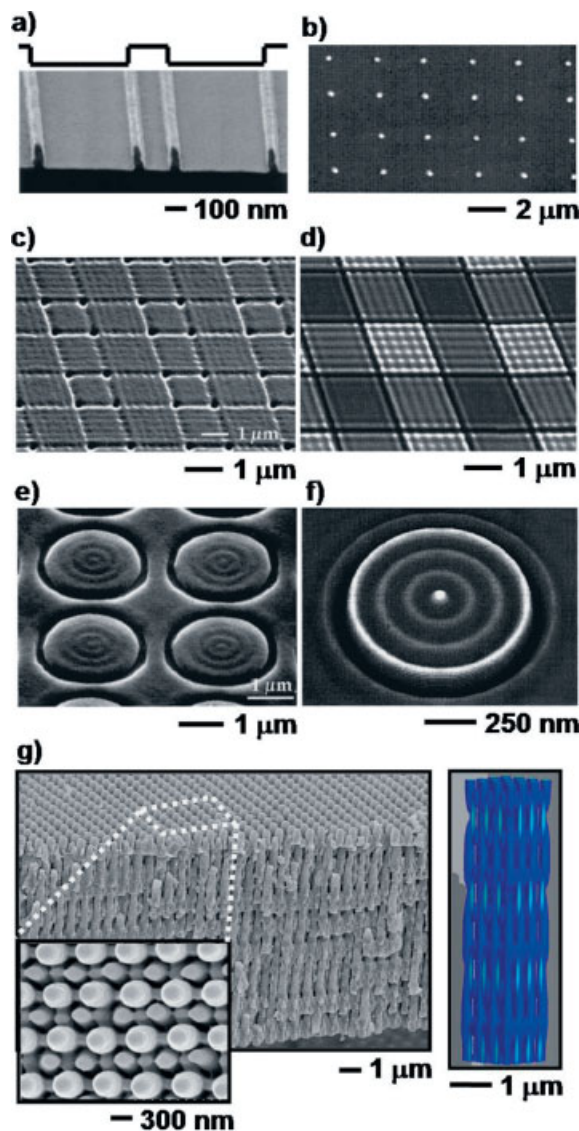


**Figure 4.** Scanning electron micrographs of typical nanostructures formed by exposure of photosensitive materials through conformable phase masks. a,b) Line and dot patterns produced by fully developing thin layer of a positive resist after single or dual exposures, respectively. c,d) Patterns and simulations, respectively, that result from dual exposure and partial development with a mask with line and space relief structure. e,f) Patterns and simulations, respectively, that result from a single exposure and partial development using a mask with raised posts of relief. g) Images (left) and simulations (right) of 3D nanostructures formed by exposure and development of a thick, transparent photopolymer using a mask with raised posts of relief.

[1] Y.-L. Loo, R. L. Willett, K. Baldwin, J. A. Rogers, *J. Am. Chem. Soc.* **2002**, *124*, 7654.  
 [2] Y.-L. Loo, R. W. Willett, K. Baldwin, J. A. Rogers, *Appl. Phys. Lett.* **2002**, *81*, 562.  
 [3] J. Zaumseil, M. A. Meitl, J. W. P. Hsu, B. Acharya, K. W. Baldwin, Y.-L. Loo, J. A. Rogers, *Nano Lett.* **2003**, *3*, 1223.  
 [4] E. Menard, L. Bilhaut, J. Zaumseil, J. A. Rogers, *Langmuir* **2004**, *20*, 6871.  
 [5] S. Jeon, J.-U. Park, R. Cirelli, S. Yang, C. E. Heitzmann, P. V. Braun, P. Kenis, J. A. Rogers, *Proc. Natl. Acad. Sci. USA*, in press.  
 [6] O. D. Velev, T. A. Jede, R. F. Lobo, A. M. Lenhoff, *Nature* **1997**, *389*, 447.  
 [7] S. A. Johnson, P. J. Ollivier, T. E. Mallouk, *Science* **1999**, *283*, 963.  
 [8] Y. A. Vlasov, X. Z. Bo, J. C. Sturm, D. J. Norris, *Nature* **2001**, *414*, 289.  
 [9] Y. Fink, A. M. Urbas, M. G. Bawendi, J. D. Joannopoulos, E. L. Thomas, *J. Lightwave Technol.* **1999**, *17*, 1963.  
 [10] F. S. Bates, *Science* **1991**, *251*, 898.  
 [11] M. Park, C. Harrison, P. M. Chaikin, R. A. Register, D. H. Adamson, *Science* **1997**, *276*, 1401.

- [12] M. Boltau, S. Walheim, J. Mlynek, G. Krausch, U. Steiner, *Nature* **1998**, 391, 877.
- [13] T. L. Morkved, P. Wiltzius, H. M. Jeager, D. G. Grier, T. A. Witten, *Appl. Phys. Lett.* **1994**, 64, 422.
- [14] H. Yang, N. Coombs, G. A. Ozin, *Adv. Mater.* **1997**, 9, 811.
- [15] C. R. Martin, *Acc. Chem. Res.* **1995**, 28, 61.
- [16] P. Hoyer, *Adv. Mater.* **1996**, 8, 857.
- [17] H. O. Jacobs, A. R. Tao, A. Schwartz, D. H. Gracias, G. M. Whitesides, *Science* **2002**, 296, 323.
- [18] H. J. J. Yeh, J. S. Smith, *IEEE Photon. Technol. Lett.* **1994**, 6, 706.
- [19] N. B. Bowden, M. Weck, I. S. Choi, G. M. Whitesides, *Acc. Chem. Res.* **2001**, 34, 231.
- [20] M. Campbell, D. N. Sharp, M. T. Harrison, R. G. Denning, A. J. Turberfield, *Nature* **2000**, 404, 53.
- [21] I. Divliansky, T. S. Mayer, K. S. Holliday, V. H. Crespi, *Appl. Phys. Lett.* **2003**, 82, 1667.
- [22] Y. Xia, J. A. Rogers, K. E. Paul, G. M. Whitesides, *Chem. Rev.* **1999**, 99, 1823.
- [23] See *MRS Bull.* **2001**, 26(7).
- [24] J. E. Smay, J. Cesarano, J. A. Lewis, *Langmuir* **2002**, 18, 5429.
- [25] A. Kumar, G. M. Whitesides, *Appl. Phys. Lett.* **1993**, 63, 2002.
- [26] C. Kim, M. Shtein, S. R. Forrest, *Appl. Phys. Lett.* **2002**, 80, 4051.
- [27] H. Schmid, H. Wolf, R. Allenspach, H. Riel, S. Karg, B. Michel, E. Delamarche, *Adv. Funct. Mater.* **2003**, 13, 145.
- [28] X. Jiang, H. Zheng, S. Gourdin, P. T. Hammond, *Langmuir* **2002**, 18, 2607.
- [29] W. R. Childs, R. G. Nuzzo, *J. Am. Chem. Soc.* **2002**, 124, 13 583.
- [30] Y.-L. Loo, J. W. P. Hsu, R. L. Willett, K. W. Baldwin, K. W. West, J. A. Rogers, *J. Vac. Sci. Technol. B* **2002**, 20, 2853.
- [31] G. S. Ferguson, M. K. Chaudhury, G. B. Sigal, G. M. Whitesides, *Science* **1991**, 253, 776.
- [32] J. A. Rogers, K. E. Paul, R. J. Jackman, G. M. Whitesides, *Appl. Phys. Lett.* **1997**, 70, 2658.
- [33] J. A. Rogers, K. E. Paul, R. J. Jackman, G. M. Whitesides, *J. Vac. Sci. Technol. B* **1998**, 16, 59.
- [34] J. Aizenberg, J. A. Rogers, K. E. Paul, G. M. Whitesides, *Appl. Phys. Lett.* **1997**, 71, 3773.
- [35] J. Aizenberg, J. A. Rogers, K. E. Paul, G. M. Whitesides, *Appl. Opt.* **1998**, 37, 2145.
- [36] H. Schmid, H. Biebuyck, B. Michel, O. J. F. Martin, *Appl. Phys. Lett.* **1998**, 72, 2379.